36. M. Dean *et al.*, *J. Biol. Chem.* **261**, 9161 (1986).
37. L. Kaczmarek, B. Calabretta, S. Ferrari, J. K. de Reil, *J. Cell. Physiol.* **132**, 545 (1987).
38. J. A. Bantle, I. H. Maxwell, W. C. Hann, *Anal. Biochem.* **72**, 413 (1976).
39. R. S. Wu, S. Tsai, W. M. Bonner, *Cell* **31**, 367 (1982); J. O. Thomas and R. D. Kornberg, *Proc. Natl. Acad. Sci. U.S.A.* **72**, 2626 (1975).
40. We wish to thank M. Peacocke, R. Miller, and B. Gilchrest for valuable discussions. Supported by a grant from NIH (AG07114). J.C. is an Established Investigator of the American Heart Association.

29 August 1989; accepted 20 November 1989

The Dominant W^{42} *spotting* Phenotype Results from a Missense Mutation in the c-*kit* Receptor Kinase

JIMMY C. TAN, KARL NOCKA, PRABIR RAY, PAULA TRAKTMAN, PETER BESMER*

The murine *white spotting* locus (*W*) is allelic with the proto-oncogene c-*kit*, which encodes a transmembrane tyrosine protein kinase receptor for an unknown ligand. Mutations at the *W* locus affect various aspects of hematopoiesis and the proliferation and migration of primordial germ cells and melanoblasts during development to varying degrees of severity. The W^{42} mutation has a particularly severe effect in both the homozygous and the heterozygous states. The molecular basis of the W^{42} mutation was determined. The c-*kit* protein products in homozygous mutant mast cells were expressed normally but displayed a defective tyrosine kinase activity in vitro. Nucleotide sequence analysis of mutant complementary DNAs revealed a missense mutation that replaces aspartic acid with asparagine at position 790 in the c-*kit* protein product. Aspartic acid–790 is a conserved residue in all protein kinases. These results provide an explanation for the dominant nature of the W^{42} mutation and provide insight into the mechanism of c-*kit*–mediated signal transduction.

THE PROTO-ONCOGENE C-*kit* ENcodes a transmembrane tyrosine protein kinase receptor which belongs to a family of receptors that includes the receptors for platelet-derived growth factor (PDGF) and colony-stimulating factor–1 (CSF-1) (*1–3*). The c-*kit* gene has recently been determined to be allelic with the dominant *white spotting* locus (*W*) on chromosome 5 of the mouse (*4, 5*). Mutations at the *W* locus affect various aspects of hematopoiesis and the proliferation and migration of primordial germ cells and melanoblasts during development (*6–8*). A large number of independent mutations are known at the *W* locus which give rise to phenotypes that vary in severity in the heterozygous and the homozygous states (*6, 9*). These distinct *W* mutations provide the opportunity to characterize both the consequences of the mutations in different cell types and the molecular basis for the developmental defects that result from them. Mutations that affect the function of the c-*kit* receptor could facilitate the definition of structure-function relations of the c-*kit* receptor in vivo.

The W^{42} allele is a dominant mutation at the *W* locus with severe effects on pigmentation, gametogenesis, and hematopoiesis. Mice homozygous for the W^{42} allele die perinatally of macrocytic anemia (*9*). Mice heterozygous for the W^{42} allele are viable, although they have severe macrocytic anemia, lack virtually all coat pigment, and their gonads are reduced in size. We determined the molecular basis of the W^{42} mutation. In mast cells of homozygous mutant mice, the c-*kit* protein product was expressed normally but displayed a defective tyrosine kinase activity in vitro. Nucleotide sequence analysis of mutant cDNAs revealed a point mutation that resulted in the substitution of an evolutionarily conserved amino acid in the kinase domain of the c-*kit* protein product.

To investigate the c-*kit* protein products in homozygous W^{42} mutant animals, we cultured mast cells from the liver of 14-day-old fetuses, that were W^{42}/W^{42}, $W^{42}/+$, or $+/+$, obtained by breeding $W^{42}/+$ animals. We showed elsewhere (*8*) that mast cells express high levels of c-*kit*, and the *W* protein product is known to be essential for fibroblast-mediated proliferation and terminal differentiation of tissue culture mast cells in the absence of interleukin-3 (IL-3) (*10*). In order to identify homozygous embryos, we determined the proliferation potential of the fetal liver–derived mast cells. One fetus (No. 9) of ten in the first litter, four of nine in the second litter, and none of seven in a third litter appeared to be homozygous, as judged from the mast cell proliferation assay (Table 1). The positive proliferation numbers can be grouped into intermediate and high values. On the basis of the proliferation potential of mast cells from $W^{42}/+$ and from $+/+$ mice, the intermediate values were derived from heterozygous genotypes and the high values from normal $+/+$ genotypes, in agreement with the dominant nature of the W^{42} mutation (Table 1).

Table 1. Proliferation of mast cells on fibroblasts. The proliferation of mast cells, derived from the liver of individual fetuses of litters generated by mating $W^{42}/+ \times W^{42}/+$ mice and from the bone marrow of adult $W^{42}/+$ and $+/+$ mice, was determined after 7 days of coculture with Balb-3T3 cells in the absence of IL-3 (*20*). $+/+$ BM, normal bone marrow; Bgd, background value is the number of round cells observed in a well containing Balb-3T3 cells with no mast cells added.

Litter 1		Litter 2	
Fetus No.	Cells per field	Fetus No.	Cells per field
1	73	12*	3
2	210	13*	3
3	64	14*	4
5	167	15	35
7	167	16	37
8	194	17*	3
9*	6	18	118
10	89	+/+ BM	115
Bgd	6	Bgd	3
$W^{42}/+$ BM	107		
+/+ BM	300		
Bgd	3		

*W^{42}/W^{42} mast cells.

Our earlier work showed that c-*kit* RNA is expressed in liver, head, and placenta of 14- to 15-day-old embryos (*8*). In order to determine whether the W^{42} mutation affects c-*kit* RNA expression, we prepared RNA from the liver, the head, and the placenta of the ten fetuses in the first litter and subjected it to blot analysis. Equal amounts of c-*kit* RNA were detected in the head and the placenta of all fetuses as well as in homozygous mutant and normal fetal liver–derived mast cells; in contrast, a lower level of c-*kit* RNA was detected in the W^{42}/W^{42} liver (No. 9) when compared with the other liver samples (Figs. 1 and 2a). These results suggest that the W^{42} mutation does not affect c-*kit* RNA expression in the fetal head, in the placenta, and in mast cells. The reduced level of c-*kit* expression in the fetal liver is in agreement with our earlier conjecture that there is a reduction of the number

J. C. Tan, K. Nocka, P. Ray, P. Besmer, Molecular Biology Program, Sloan Kettering Institute and Cornell University Graduate School of Medical Sciences, New York, NY 10021.
P. Traktman, Cell Biology Department and Molecular Biology Program, Cornell University Graduate School of Medical Sciences and Medical College, New York, NY 10021.

*To whom correspondence should be addressed.

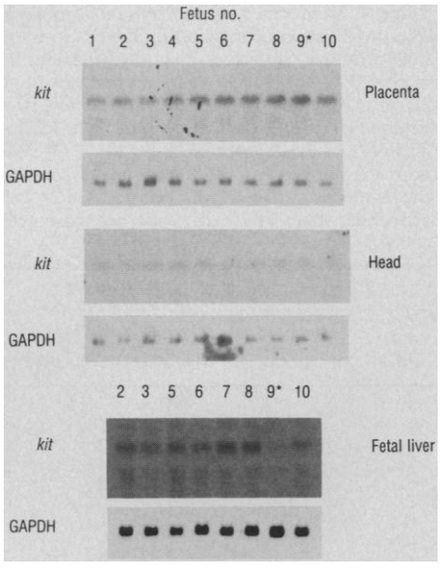

Fig. 1. Expression of c-*kit* RNA transcripts in W^{42}/W^{42} fetal tissues. RNA was prepared from the head, the liver, and the corresponding placenta of ten 14-day-old fetuses (obtained by breeding $W^{42}/+$ with $W^{42}/+$ mice) and analyzed by agarose gel electrophoresis and blot hybridization (*21*). Total RNA was used and hybridization was done with a c-*kit* cDNA probe. Hybridization with a GAPDH (glyceraldehyde phosphate dehydrogenase) probe is shown to indicate equal loading.

of c-*kit* expressing cells in this tissue because of lack of c-*kit* function (*8*).

We then analyzed the c-*kit* protein products in mast cells derived from the livers of individual fetuses to determine whether the structural features of the c-*kit* protein or its functional properties are affected by the W^{42} mutation. Immunoprecipitates obtained from extracts of [^{35}S]methionine-labeled mast cells were analyzed by SDS–polyacrylamide gel electrophoresis (SDS-PAGE) (Fig. 2). Structurally, the 160- and the 130-kD forms of the c-*kit* protein in W^{42}/W^{42} and in +/+ or $W^{42}/+$ mast cells do not differ in size or relative amount, and their metabolic stabilities are similar as well (*11*). The 160-kD form of the c-*kit* protein contains complex carbohydrate modifications and is thought to represent the cell membrane form of the protein (*3*). Cell surface expression of c-*kit*–encoded antigens was investigated by flow cytometry (Fig. 2c). Comparable levels of membrane fluorescence in the mutant and nonmutant mast cells suggested that similar amounts of the c-*kit* protein are expressed on the cell surface of homozygous mutant and normal mast cells. To determine whether the c-*kit*–associated autophosphorylation activity is affected by the W^{42} mutation, we performed immune complex kinase assays. Equal amounts of extract, prepared from identical cell samples of fetal liver–derived mast cells as used in the above metabolic labeling experiment, were immunoprecipitated with antibody to c-*kit* and incubated with [γ-^{32}P]ATP (adenosine triphosphate) in a kinase reaction; the reaction products were analyzed by SDS-PAGE. Autophosphorylation activity was observed in samples derived from +/+ or $W^{42}/+$ mast cells (Nos. 1 to 8, 10, 15, 16, 18, and 19; Fig. 2c), but in all of the mast cells from homozygous mutant mice that we had analyzed (Nos. 9, 12, and 13), the autophosphorylation activity was significantly reduced (Fig. 2c; fetus 12 is not shown). These results indicate that the c-*kit*^{W42} protein (in the discussion below, c-*kit* DNA, RNA, and protein of the W^{42} allele are referred to as c-*kit*^{W42}) is indistinguishable from the wild-type c-*kit* protein with regard to size and cell surface expression, but that it has defective in vitro kinase activity. This result furthermore suggests that the W^{42} mutation is located in the c-*kit* coding sequence.

To identify the W^{42} mutation, we determined the nucleotide sequence of the c-*kit*^{W42} coding region by using the reverse transcriptase (RT) modification of the polymerase chain reaction (PCR) (*12*) (Fig. 3). The c-*kit* coding region was divided into five overlapping subregions for PCR amplification, and primers were made accordingly (*13*). Total RNA from the head of homozygous mutant embryos and from the brain of a 2-week-old C57BL/6 mouse, as a control, were used as template for cDNA synthesis and PCR amplification (*14*). The amplified DNA fragments were subcloned into M13mp18 and M13mp19, and their sequence was determined. Comparison of the wild-type with the c-*kit*^{W42} sequence indicated one point mutation at position 2396 (G to A) of the known c-*kit* cDNA sequence, which results in the change of aspartic acid at position 790 to asparagine. This mutation was confirmed by repeating the RT-PCR amplification and the sequence determination on both fetal brain and mast cell RNA samples. Asp^{790} is a conserved residue in all tyrosine and serine-threonine kinases, as well as in bacterial phosphotransferases, and is thought to be important in the phosphate transfer reaction (*15–17*). Mutation of Asp^{790} to Asn likely affects the c-*kit*^{W42} kinase, and this prediction is in agreement with the observed defective kinase activity of the c-*kit*^{W42} protein in vitro. With the Fujinami sarcoma virus P130$^{gag\text{-}fps}$ tyrosine kinase, substitution of the equivalent aspartic acid residue of the *fps* kinase by asparagine abolishes kinase activity in vitro, in agreement with our result (*17*).

Molecular analysis of c-*kit* in *W* mutant

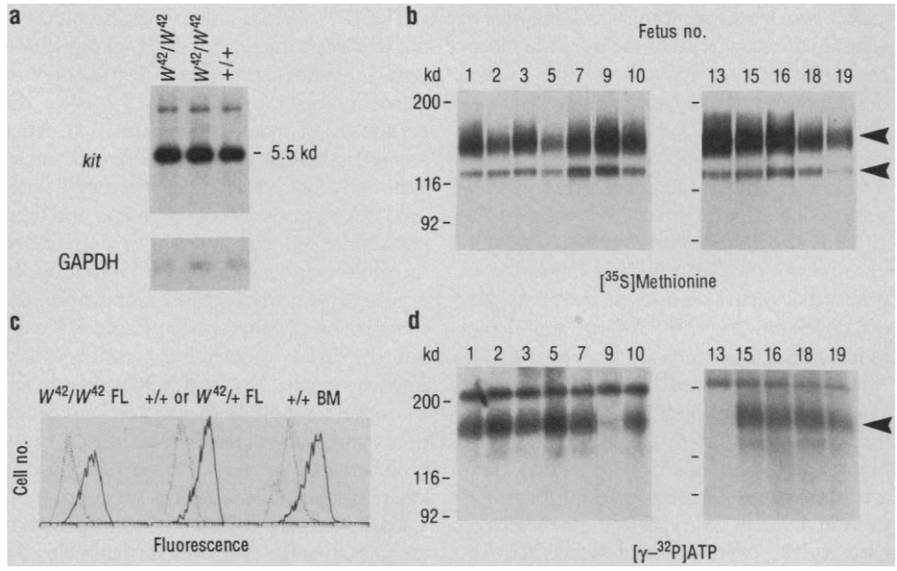

Fig. 2. Expression of c-*kit* RNA, protein, and protein kinase activity in fetal liver–derived W^{42}/W^{42} mast cells. (**a**) Expression of c-*kit* RNA transcripts in normal and in homozygous mutant mast cells. RNA prepared from mast cells (1 μg per lane) was electrophoretically separated, blotted, and hybridized with a c-*kit* cDNA probe as described in Fig. 1. (**b**) Immunoprecipitation analysis of c-*kit* protein products. Extracts made from metabolically labeled mast cells derived from individual fetuses were immunoprecipitated with antibody to c-*kit* and analyzed by SDS-PAGE (*22*). (**c**) Determination of cell surface expression of c-*kit* protein detected by flow cytometry (*23*). Labeling with antibody to c-*kit* is indicated with a solid line and labeling with preimmune rabbit serum with a dotted line. (**d**) Determination of in vitro kinase activity of c-*kit* protein in mast cells. Cell lysates prepared from equivalent amounts of protein of unlabeled mast cells derived from individual fetuses were immunoprecipitated with antibody to c-*kit*, processed for autophosphorylation reactions with [γ-^{32}P]ATP and the reaction products then were analyzed by SDS-PAGE (*22*). Arrows indicate the relative mobility of c-*kit* protein products. Protein size markers are indicated in kilodaltons.

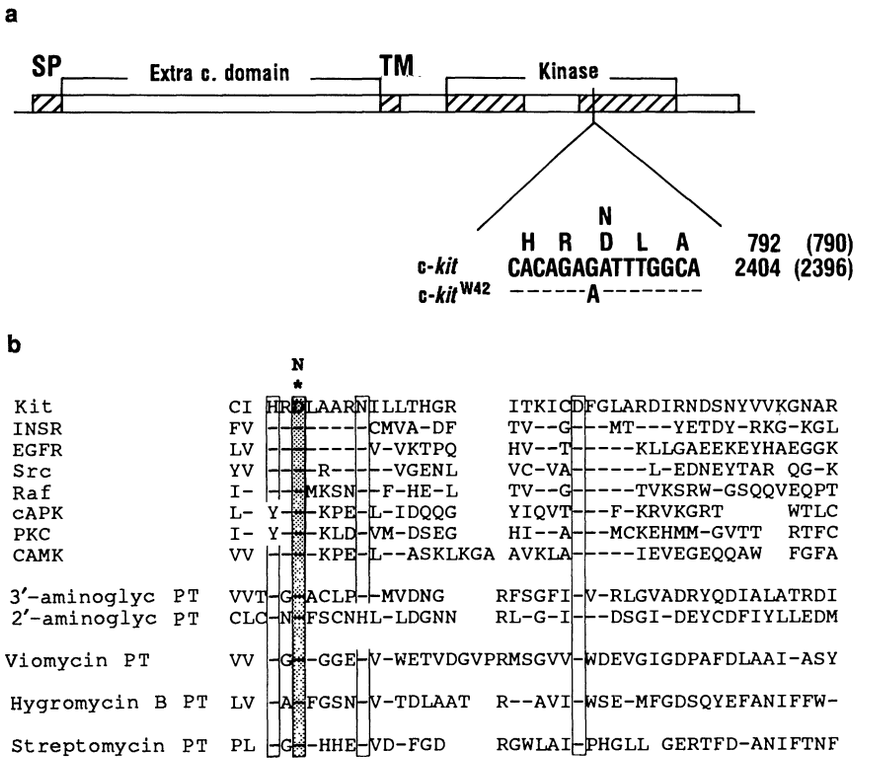

Fig. 3. Determination of the c-*kit*^{W42} mutation. The coding sequence of c-*kit*^{W42} was cloned by using RT-PCR and the nucleotide sequence determined (*13, 14*). (**a**) Schematic representation of the point mutation at position 2396. (**b**) Comparison of c-*kit* amino acids 786 to 828 with the corresponding sequences of the following tyrosine and serine/threonine kinases and bacterial phosphotransferases (PTs): insulin receptor (INSR), EGF receptor (EGFR), c-*src* protein product (Src), c-*raf* protein product (Raf), adenosine 3′,5′-monophosphate–dependent protein kinase (cAPK), protein kinase C (PKC), calmodulin-dependent protein kinase (CAMK), 3′-aminoglycoside phosphotransferase, 2′-aminoglycoside phosphotransferase, viomycin phosphotransferase, hygromycin B phosphotransferase, and streptomycin phosphotransferase. Amino acid identities are indicated by a dash. Abbreviations for the amino acid residues are: A, Ala; C, Cys; D, Asp; E, Glu; F, Phe; G, Gly; H, His; I, Ile; K, Lys; L, Leu; M, Met; N, Asn; P, Pro; Q, Gln; R, Arg; S, Ser; T, Thr; V, Val; W, Trp; and Y, Tyr.

mice previously indicated a large chromosomal insertion and a functionally altered gene product as the bases for *W* mutations (*5, 8*). We show that the W^{42} allele is the result of a point mutation that affects the c-*kit*–associated tyrosine kinase, but not the size and the cell surface expression of the c-*kit*–encoded protein.

The W^{19H} mutation is the result of a 2- to 7-cM chromosomal deletion that includes c-*kit* and thus represents a c-*kit* null mutation with lack of protein function (*4, 5, 18*). Heterozygous W^{19H} animals display minimal white spotting, have no pigment dilution, and are not anemic. The strong mutant phenotype of W^{42}/+ heterozygotes, therefore, appears to reflect an interaction of the mutant allele with the normal allele. Ligand-induced transmembrane signaling of receptor tyrosine kinases is thought to involve the formation of receptor oligomers (*19*). We presume that signal transduction induced by the ligand of the *kit* protein involves receptor oligomerization as well. Therefore, the mutant c-*kit*^{W42} protein in receptor heterodimers could interfere with *kit* ligand-induced signal transmission, and this would effectively result in a significant reduction of the number of functional c-*kit* receptors on the cell surface and thus explain the severe effects of the phenotype in heterozygous W^{42}/+ animals. In addition, the mutant c-*kit* protein may compete for ligand. Our evidence of a point mutation in c-*kit*^{W42}, which inactivates the c-*kit* kinase and does not affect the size or the cell surface expression of the protein, is in agreement with the proposed mechanisms. The c-*kit*^{W42} mutation then has the features of a dominant loss-of-function mutation with respect to the known pleiotropic functions of c-*kit*.

A function in cell differentiation and development is not known for many mammalian kinase receptors. Mutations in these receptor genes, like *W* mutations might be recessive lethals or dominant loss-of-function mutations. The construction of dominant receptor mutations similar to c-*kit*^{W42} and the production of transgenic or chimeric mice may provide a means to define the roles of these receptor systems in development.

REFERENCES AND NOTES

1. P. Besmer *et al.*, *Nature* **320**, 415 (1986).
2. F. Qiu *et al.*, *EMBO J.* **7**, 1003 (1988).
3. S. Majumder, K. Brown, F. Qui, P. Besmer, *Mol. Cell. Biol.* **8**, 4896 (1988).
4. B. Chabot, D. A. Stephenson, V. M. Chapman, P. Besmer, A. Bernstein, *Nature* **335**, 88 (1988).
5. E. N. Geissler, M. A. Ryan, D. E. Housman, *Cell* **55**, 185 (1988).
6. E. S. Russell, *Adv. Genet.* **20**, 357 (1979).
7. W, K. Silvers, *The Coat Colors of Mice* (Springer-Verlag, New York, 1979), pp. 206–241.
8. K. Nocka *et al.*, *Genes Dev.* **3**, 816 (1989).
9. E. N. Geissler, E. C. McFarland, E. S. Russell, *Genetics* **97**, 337 (1981).
10. J. Fujita *et al.*, *J. Cell. Physiol.* **134**, 78 (1988).
11. K. Nocka, unpublished results.
12. E. S. Kawasaki *et al.*, *Proc. Natl. Acad. Sci. U.S.A.* **85**, 5698 (1988).
13. Oligonucleotide primers for PCR amplification were as follows: Sense primers (5′ to 3′) primer 1 (1 to 24) ATGGAATTCAGAGTCTAGCGCAGC-CAC; primer 3 (561 to 590) GCGCCTAC-CACCGGATCCGTGTCCGCTGTG; primer 5 (1161 to 1186) ATGGAATTCGCCTGACCA-GATTAAAA; primer 7 (1750 to 1771) ATGGA-ATTCCTTATGATCACAAATGG; primer 9 (2228 to 2257) ACAGACAAGAGGGGATCCGCAAGA-ATAGAC. Antisense primers (3′ to 5′) primer 2 (665 to 636) AGTTTCACGCCCTTCGAAAGTT-CCGATAGG; primer 4 (1239 to 1210) GAAAGA-CCACAGCTTAAGACTACGGTCACG; primer 6 (1834 to 1805) TGTAACCCTCGACCTAGGAA-GCCCTTCCAG; primer 8 (2325 to 2296) TCTACTGCTCGACCTAGGCCTGGACCTACT; primer 10 (3063 to 3034) GGGAAACTGAACTT-AAGATAAGGTCCCATC.
14. The RT-PCR amplification was carried out essentially as described (*11*). For cDNA synthesis, 10 μg of total embryo head RNA in 50 μl of 0.05*M* tris, *p*H 8.3; 0.075*M* KCl; 3 m*M* $MgCl_2$; 10 m*M* dithiothreitol; 200 μ*M* deoxyribonucleotide triphosphates (dNTPs); and RNasin (1 unit per microliter) (Promega) was incubated with 100 pmol of antisense primer and Moloney murine leukemia virus reverse transcriptase at 42°C. The cDNA was amplified by using 2.5 units of *Taq* DNA polymerase and 100 pmol of sense primer in 100 μl of 50 m*M* KCl; 10 m*M* tris, *p*H 8.3; 1.5 m*M* $MgCl_2$; and 0.01% (w/v) gelatin and 25 to 30 cycles in an automated thermal cycler (Perkin-Elmer Cetus). The amplified fragments were purified by agarose gel electrophoresis, digested with appropriate restriction enzymes, and subcloned into M13mp18 and M13mp19 for sequence analysis [F. Sanger, S. Nicklen, A. R. Coulson, *Proc. Natl. Acad. Sci. U.S.A.* **74**, 5463 (1977)].
15. S. K. Hanks, A. M. Quinn, T. Hunter, *Science* **241**, 42 (1988).
16. S. Brenner, *Nature* **329**, 21 (1987).
17. M. F. Moran, C. A. Koch, I. Sadowski, T. Pawson, *Oncogene* **3**, 665 (1988).
18. M. F. Lyon *et al.*, *Genet. Res.* **44**, 161 (1984).
19. Epidermal growth factor (EGF)– and PDGF-induced receptor activation is believed to be facilitated by receptor dimers [Y. Yarden and J. Schlessinger, *Biochemistry* **26**, 1443 (1987); C-H. Heldin, A. Ernlund, C. Rorsman, L. Ronnstrand, *J. Biol. Chem.* **264**, 8905 (1989)].
20. Mast cells from livers of individual day 14 fetuses obtained by mating W^{42}/+ × W^{42}/+ mice and from the bone marrow of adult W^{42}/+ and +/+ mice were grown in IL-3–containing medium (WEHI-3–conditioned medium). Mast cells were washed free of IL-3 and plated on a feeder layer of irradiated (2000 rads) confluent Balb-3T3 cells in 24-well plates at 10^4 cells per well. After 7 days of culture, mast cells were counted as round, viable cells at a magnification of ×200. Ten ×200 microscope fields or 500 cells were counted for each point, and the data are expressed as number of cells per field. Staining with toluidine blue indicated that >95% of all round cells were mast cells.
21. Tissues were homogenized in guanidinium isothiocyanate, and RNA was isolated according to the method of Chirgwin (J. M. Chirgwin, A. E. Przybyla, J. R. Macdonald, W. J. Rutter, *Biochemistry* **18**,

5294 (1979)]. Total cellular RNA (10 to 15 μg) was fractionated in 0.7% agarose-formaldehyde gels, transferred to nylon membranes (Nytran, Schleicher and Schuell), and prehybridization and hybridization were performed as previously described [(*8*); H. Lehrach, D. Diamond, J. M. Wozney, H. Boedtker, *Biochemistry* **16**, 4743 (1978)]. The murine c-*kit* cDNA labeled with [^{32}P]phosphate, prepared by the random primer method, was used as a probe for hybridization [A. P. Feinberg and B. Vogelstein, *Ann. Biochem.* **132**, 6 (1983)].

22. Mast cells were labeled with [^{35}S]methionine for 5 hours and Triton X-100 lysates were prepared. Equal amounts of trichloroacetic acid precipitable counts were immunoprecipitated with rabbit antisera to c-*kit* conjugated to protein A–Sepharose and analyzed by SDS-PAGE (10%), and autoradiography as previously described (*8*). Immune complex kinase reactions were performed essentially as described (*3, 8*); equal numbers of cells were lysed in Triton X-100 and immunoprecipitated as above. Kinase reactions were carried out in 30 μl of 20 m*M* 1,4-piperazinediethanesulfonic acid (Pipes) (*p*H 7.2), 10 m*M* $MnCl_2$, 10 μ*M* ATP, 20 μ*M* sodium vanadate, and 20 μCi of [γ-^{32}P]ATP for 10 min at 30°C.

23. Flow cytometry was performed by labeling mast cells with kit antisera specific for extracellular determinants of c-*kit*. The antiserum to c-*kit* was obtained by immunization of rabbits with a recombinant vaccinia virus expressing the c-*kit* protein product (a detailed description of this reagent will be published elsewhere). Mast cells were labeled with preimmune and immune sera in phosphate-buffered saline (PBS) containing 5% bovine serum at 4°C for 30 min, washed, and labeled with fluorescein isothiocyanate (FITC)–conjugated goat antiserum to rabbit immunoglobulin G (Becton Dickinson). Cells were then washed and fixed in 1% paraformaldehyde in PBS and analyzed with a flow cytometer (FACSCAN, Becton Dickinson). Dead cells were gated out on the basis of forward and 90° light scatter; results are expressed as cell number (linear scale) versus fluorescence (log scale).

24. We thank the Viral Oncology Group and O. Rosen for their advice, continued interest, and discussions and E. Chiu for excellent technical assistance. Supported by grants from the American Cancer Society and from the National Cancer Institute, R01-CA-32926 and P01-CA-16599 (to P.B.).

8 August 1989; accepted 2 November 1989

Localization of an Acetylcholine Receptor Intron to the Nuclear Membrane

STEPHEN A. BERMAN, SHERRY BURSZTAJN, BARBARA BOWEN, WALTER GILBERT

The first intron of the RNA for the acetylcholine receptor (AChR) α subunit shows a ringlike distribution around nuclei in multinucleated myotubes by in situ hybridization. This pattern is not observed for an actin intron or U1 RNA. Quantitation of the intron sequences reveals large variations in the amount of both the AChR and actin introns between nuclei within the same myotube, although all nuclei express equivalent amounts of U1 RNA. This differential RNA expression indicates that nuclei can individually control expression of messenger RNAs. The restricted distribution of the AChR intron RNA suggests a previously unknown step in RNA processing.

IN SITU HYBRIDIZATION WITH DNA probes can reveal the distribution of mRNA in cultured cells. When embryonic chick myoblasts are cultured, they fuse to produce multinucleated myotubes, which spontaneously contract. Studies on the distribution of mRNA for the α subunit of the AChR, an essential component of the neuromuscular junction, have shown that nuclei in the same myotube differ in their expression of this transcript (*1–3*). We have used a probe for the first intron of the AChR α subunit mRNA (*4*) in such an in situ hybridization experiment with skeletal muscle cells from 11-day-old chick embryos. We hybridized the myotubes 4 days after plating with a highly radioactive, single-stranded DNA probe. After autoradiography, we stained the preparation with bisbenzamide and visualized the nuclei and the silver grains simultaneously by fluorescence and dark-field microscopy (*5*). A ringlike distribution of grains, confined to the periphery of the nuclei, was observed (Fig. 1, A to C). The peripheral distribution of grains was more apparent in dark-field images (Fig. 1B), with the centers of the nuclei being almost completely devoid of silver grains.

To confirm that this peripheral distribution of grains was not due to a permeability barrier, we hybridized the cells with a probe of comparable length for U1 small nuclear RNA (*6*), a member of a class of small RNAs that are present in the nucleus complexed with certain proteins to form small nuclear ribonucleoproteins (snRNPs) (7). In situ hybridization studies have shown that the U1 RNA is present in the nucleus with no preferential intranuclear localization (*8*). The U1 probe labeled all nuclei in the myotubes with a homogeneous distribution of grains (Fig. 1G).

As a further control, we hybridized the cells with a probe of similar length corresponding to the fifth intron (intron E) of chicken cardiac α actin, one of the most abundant actin species expressed during embryonic myotube development (*9*). The actin intron probe produced a pattern of silver grains confined diffusely to the nuclei (Fig. 1, D to F). Exon probes for both the AChR α subunit (Fig. 1H) and actin (Fig. 1I) mRNAs produced a homogeneous distribution of grains that was confined within the cytoplasm of the muscle cells. Because the labeling and exposure times were the same for all the probes, there would appear to be comparable amounts of actin and AChR α subunit mRNAs and introns.

A quantitative analysis of silver grain distribution revealed heterogeneity in the degree of nuclear labeling. An examination of 463 nuclei, identified with bisbenzamide, from three different cultures that were hybridized with the AChR α subunit intron probe showed that 21% of the nuclei had more than ten grains per nucleus, whereas 20% of nuclei were either devoid of grains or had less than two grains (Fig. 2A). Cells hybridized with the actin intron probe also showed variability among nuclei; however, the grain distribution was very broad and 90% of nuclei had more than ten grains per nucleus (Fig. 2B). In contrast, cells hybridized with the U1 RNA probe showed a uniform grain distribution among nuclei, with 99% of nuclei having greater than ten grains and none possessing less than two grains (Fig. 2C). The background counts in each of these experiments were equivalent to 0.2 to 0.3 grains per nucleus (*10*).

The localization of the AChR α subunit intron (or the entire pre-mRNA) to the periphery of the nucleus represents a regionalization of transcripts of a type not seen before. The U1 probe labels the nucleoplasm of all nuclei without noticeable intranuclear regionalization. This shows that the nuclei are penetrable by the probes and that all nuclei are functional. The general nuclear localization of the actin intron further shows that the ring localization is an unusual feature of the AChR α subunit intron. The pattern seen with the AChR α subunit intron resembles the peripheral labeling described by Hutchison and Weintraub (*11*) after their in situ nick translation of the exposed chromatin in mouse L cells; they hypothesized that an exposed peripheral region of nuclei was the site of transcription. However, the rings in our experiments are unlikely to be a direct indication of transcription of the AChR α subunit gene because only two copies of the gene exist in

S. A. Berman, Department of Neuro-oncology, M. D. Anderson Hospital, 1515 Holcombe Boulevard, Houston, TX 77030.
S. Bursztajn, Departments of Neurology and Cell Biology, Baylor College of Medicine, Houston, TX 77030.
B. Bowen and W. Gilbert, Department of Cellular and Developmental Biology, Harvard University, Cambridge, MA 02138.